SCHOOL OF MECHANICAL, AEROSPACE AND AUTOMOTIVE ENGINEERING

IMechE UAS Challenge: Thrust Vectoring as an Alternative Control Mechanism for a Hybrid UAV

302MAA – INDIVIDUAL AEROSPACE PROJECT

Student Name: Miguel Ponce Argilés

SID: 11609342

Supervisor: Dr. Rashid Ali

11th April 2022

Abstract

In this paper the complete Final Year Project is presented. Aims and objectives are set in the introduction, and they are referred in to in latter sections when achieved. The project starts with the literature review, which sets a base knowledge from which to start developing the project. Then, the methodology followed is described, covering powerplant configuration, battery life and the most crucial part of the project: transition to forward flight modelling and simulation. This presents a major challenge, and a *Matlab* program is created to develop two different transitions: *Transition I* and *Transitions II*. Then, the results are plotted and analyzed in the section of results, analysis and discussion. Lastly, some import conclusions are drawn, and future work is presented to the reader.

Index

1. Introduction

In the course of their history, Unmanned Aerial Systems (UAS) development has been mainly driven by applications in the military field, being the civil and the rest of fields behind in terms of technology mostly due to a lack of a framework of regulations. Thus, the UAS full potential is yet to be demonstrated (Valavanis, 2009, p. 1). Presently, a broad market is rising given their wide range of potential applications. Their versatility ranges from surveillance and reconnaissance, humanitarian and environmental missions, infrastructure inspection, tracking operations and delivery services among many others. Furthermore, this emerging generation of drones fulfills their purpose at a small size and an inexpensive cost (Bestaoui, 2018, p. 1).

In the IMechE UAS Challenge, teams of students work together to develop a full design and build cycle of an UAS. The UAS is expected to operate autonomously while completing several tasks such as area search, waypoint navigation and accurate 'Aid Package' delivery. This mission imitates the real-world scenario in which a natural disaster has occurred, and it is crucial to supply the affected population with humanitarian aid of food, shelter and first aid supplies at the earliest from the nearest Rescue Centre. In order to accomplish so, a Vertical Take-Off and Landing (VTOL) type aircraft has been deemed the most appropriate. The reasons underlying this choice is the VTOL's ability to take-off and land anywhere, and most importantly its ability to hover in mid-flight to deliver the payload safely and accurately. Moreover, this does not have a penalty in cruise flight as it is able to transition from hover to forward flight to become a conventional aircraft.

The project is divided into various roles: aerodynamics, stability and control, autopilot, structures and CAD design, powerplant and thrust vectoring, simulation, payload release, and image recognition. The individual progress in each of the fields will result in the completion of the UAS' design. This report is focused in the powerplant and thrust vectoring.

For this project's completion, 3 aims have been established and 2 objectives set to help fulfill each aim. The success of the project will be based on this. These aims and objectives are:

- Aim *A1*: Explore thrust vectoring as a mechanism for control.
  - Objective *O1-A1*: Explore suitable mechanisms to allow control of a hybrid UAV.
  - Objective *O2-A1*: Determine precisely how pitch, roll and yaw control will be achieved.
- Aim *A2*: Implement thrust vectoring in the hybrid UAS.
  - Objective *O1-A2*: Configure a powerplant to satisfy or exceed competition's requirements.
  - Objective *O2-A2*: Study, calculate and simulate the transition from hover to forward flight and vice versa.
- Aim *A3*: Take part in the IMechE UAS Challenge.
  - Objective *O1-A3*: Help designing and manufacturing the hybrid UAS. The design includes powerplant configuration in relation with the rest of the subsystems (specially from an aerodynamic viewpoint) as well as the interrelationship between the other subsystems.
  - Objective *O2-A3*: Help coordinate flight maneuvers, stability, and control: Autopilot integration.

2. Literature Review

2.1. Thrust vectoring

The interest of the aerospace sector in thrust vectoring is justified given the numerous advantages it offers: better maneuverability, performance and stealth among others. However, its implementation has proven to be a challenge because of the mechanism's complexity and heavy weight. Thrust vectoring is basically a controlled change in the direction of the thrust produced by an engine, which can be achieved in various ways. The most popular approach in the aviation industry is to obtain the deflection of thrust by altering the configuration of the engine exhaust nozzle. In this category falls the traditional mechanical thrust vectoring, exemplified by the experimental aircraft F/A-18 HARV; and fluidic thrust vectoring, in which fluid-dynamic interactions are used to control the flow. This subcategory encloses several technologies and some of them have been successfully tested in the laboratory but are yet to be implemented in a real aircraft (Kowal, 2002, p. 145-147).

There are, however, other ways to achieve thrust vectoring that are more suitable to the project as the competition allowed powerplant consists in electrical motors with a propeller. For instance, if the motors were fixed on the wings there could be a mechanism that tilted the wing so that thrust vectoring was achieved. Nevertheless, the mechanism that would allow that would have to be quite complex and strong, which would add extra weight. The best possible solution would be to tilt the rotors alone, leaving the wing fixed. This is known as a tiltrotor, and a great example in this category is the V-22 Osprey, which was the first production tiltrotor aircraft.

Single-axis rotation change the thrust direction vertically and can replace or complement horizontal control surfaces, while multi-axis rotation can vector thrust in any direction and therefore replace or complement both vertical and horizontal control surfaces (Kowal, 2002, p. 146). For this project, it will suffice with the single-axis rotation, allowing pitch control of the UAS. In addition, it can be attempted to obtain yaw control by altering the thrust of a propeller relative to the other.

With this, Objective *O1-A1* is achieved.

2.2. Ducted Propeller Configuration

A ducted propeller is a configuration in which the propeller is surrounded by an encasing, which is called a duct. The interest in this configuration relies in two features: the safety it provides, and the increased thrust produced at low velocities. This is why this configuration has grown popular in small VTOL UAVs (Abdessameud, 2013, p. 24), which perfectly fits the conceptual design of the project. It can also help reducing the damage to the propeller and motor in the event of a crash, which are the most expensive and difficult to repair parts of an aircraft.

The aerodynamics regarding the thrust increase will be addressed next. When the propeller starts rotating, it creates a pressure distribution over the area of the blades, having different pressures at the upper and lower side of the blades. This pressure difference tends to being equalized, and it generates a flow at the blade tips (just as the induced drag in an aircraft wing) which generates vortices that decrease the propellers efficiency. By mounting an encasing or shroud around the propeller, this effect is greatly mitigated and the propeller greatly increases its efficiency. This is especially true when hovering or at small velocities (Roberts, 2007, p. 2). This characteristic makes it particularly interesting for the project, although it also has to be taken into account some negative aspects. For instance, it is a structural challenge as it is not simple to manufacture. In addition to that, it will add weight and drag to the UAS, which is not desirable. Therefore, it is necessary to carefully study if the trade-off is beneficial for this particular case. This approach will later be discarded due to the outweigh of downsides.

2.3. Flight dynamics: Vertical Climb and Descent

When climbing or descending vertically, the duct experiences airflow because of the movement added to the induced velocity by the propeller. In the climb, airflow caused by the vertical movement and the induced velocity are combined since both have the same direction. However, during descent the directions are opposite: airflow moves upwards while induced velocity keeps pointing to the ground. This creates a turbulent flow that is out of the scope of the momentum theory. The mathematics behind this phenome need to be addressed in further research (Roberts, 2007, p. 17).

2.4. Flight dynamics: Hover Flight & Transition

The nature of the front propeller tilting mechanism will have a big impact in the dynamics of every phase of flight. This is true because the rotation of the propeller and motor combination implies a horizontal movement of these components, and since they have a mass the center of gravity of the aircraft will be displaced. Not only that, but the thrust of the three motors will have to be adjusted depending on the position and angle of the front propeller in order to achieve equilibrium of moments about the center of gravity (i.e. stability in the pitch axis) as well as to provide the necessary lift (vertical thrust) to overcome the weight of the aircraft at the same time. This case commented will prove to be a challenge in the transition flight phase, until enough horizontal velocity is gained to generate sufficient lift with the wings to maintain the UAS aloft. The equations governing the dynamics of these flight phases are presently being investigated and will be detailed in later works.

Having stated this, some jet induced effects occurring in and out of ground effect should be explored for both hover and transition, as they are responsible for lift losses that are not be neglected (Kuhn, 2006, p. 6-9). Empirical and CFD methods may be used to determine the extent of this effects to the projects' aircraft.

3. Methodology

In this section it will be described the approach taken to conduct the research. A crucial part of the project to define in advance due to the dependance it has in other roles of the UAV design is the powerplant configuration.

3.1. Powerplant Configuration

As stated in earlier work, the powerplant configuration will consist in three electric motors with their appropriate propellers, two mounted on the wings and one mounted on the nose of the UAS. Evidently, the front motor will have a pull propeller given its location. Further research and discussion amongst team members and supervisor has shown the two single-axis 90 degrees rotation wing propellers to be too complex of an alternative, if not unachievable provided the available means. Two robust tilting mechanisms would have to be designed and placed in the internal structure of the wing to avoid upsetting the aerodynamics in forward flight, which would result in a thicker lower wing which in turn has an aerodynamic penalty in forward flight as well. In addition to that, the difficulty in the transition flight phase would be notably increased because there is an extra independent variable to the equation: the wing propellers' tilting angle. As an engineer design simplicity is sought, so if the same outcome (VTOL capabilities while behaving as a conventional aircraft in cruise flight) can be achieved in a simpler manner, it is often the right choice. This way manufacturing, assembly and maintenance will be easier tasks.

The powerplant will therefore be configured as it follows: two fixed propellers mounted on the wings to provide the vertical take-off and landing; and a pull propeller with a single-axis 95-degree rotation to provide vertical take-off and landing and pitch control throughout every phase of flight mounted on the nose of the UAS. Horizontal and vertical control surfaces will be present in the UAV to achieve roll and yaw control and for redundancy in the pitch control. With this Objective *O2*-A1 is accomplished. Moreover, the two wing motors may be used to provide extra lift in cruise flight if the wings do not generate enough lift to overcome the weight of the aircraft. However, in the ideal scenario the wing motors should be switched off or kept to a minimum RPM (to increase circulation around the wing) during cruise flight to cut on drag. The front propeller range of rotation is explained by its two tasks: 0–90-degree range for VTOL performance (propeller in horizontal position to take-off and land and in vertical position to provide thrust for cruise flight); and 85–99-degree range to provide pitch control. This will be achieved by means of a mechanism that will rotate the propeller as it moves along with a support aligned with the longitudinal axis of the plane so as to avoid contact between the blades and the nose of the aircraft when pointed in the upwards direction.

The ducted propeller was previously proposed to gain thrust performance at low speeds. In this configuration there is no pressure losses as a result of air flowing around the blade tips due to the pressure difference generated, so a wider propeller towards the tip could be used. This described is a fan-type propeller, but it has nevertheless been ruled out of the design for the next reasons:

- Fan-type propellers are bulkier, and as they are to be integrated in the wings it would result in thicker wings, which would be detrimental for the UAS' aerodynamics and weight.
- Lack of available performance data.
- Lack of wide range of commercial options for aircrafts.

Therefore, a conventional two-blade propeller will be used for every motor. This does not mean, however, that the wing propellers will not be shrouded. In fact, their integration in the wing will provide the shrouding. This might create a problem in determining the thrust of the wing propellers precisely and consequently in achieving longitudinal stability in hover and transition. As per the motor and propeller selection, this gain in thrust is not considered, but will be evaluated by testing. This matter will be further addressed in future work.

Calculations have been done to determine the powerplant required. Initially, the three electric motors were expected to have similar specifications rather than a more powerful motor at the front, but this decision was overruled as it makes more sense to have a more powerful motor at the front to make the most out of the power installed in the UAV. Since this front motor will be used throughout the full flight, it will be the more capable. Otherwise, there would be a "waste" of power in the wing motors, switched off during most of the flight. The UAS will have an estimated take-off weight of 10 kg, so the three motors together will have to generate about 100 N of thrust in hover. However, the UAS will also need to climb vertically to a safe distance, so the total thrust to weight ratio is set to 1.2, which yields a total thrust of 120 N. In forward flight only the front motor is switched on, and a common figure of thrust to weight ratio is 0.5-0.6 to ensure decent acceleration. Given this, the front motor will be set to produce around 6 kg of thrust (60 N), while the wing motors will be set to approximately 3 kg each.

Then, the search for a motor and propeller combination to achieve the thrust requirements was conducted. A database was created to compare the commercially available motors in the range of 500-1500 W, and the maximum power to weight ratio was used as a parameter to select a motor within the motors that complied with the thrust requirements.

The motor *Tornado Thumper 5055/06* was found to be an ideal option for the front motor at 1280 W of output power. Combined with a 17x6E propeller, it can produce up to 58.9 N of thrust in stationary while maximizing the output power of the motor at 8000 RPM. A reasonable cruise speed to assume in 15 m/s, at which it can produce 36 N of thrust to counteract the equal and opposed drag.

For the wing motors, an extra constraint was set: it had to be thin enough to fit in the wing and not stick out from the top or bottom, otherwise this would incur in extra drag in forward flight. For this purpose, the flat motor *Cobra CM-4510/28 Multirotor* was selected for the wings. This is a 780 W motor with a body length of 32.8 mm that easily fits in the wing. The fitting and location in the wing were done in collaboration with the person responsible for designing the wing structure, and the motor with the propeller had expected fit in the wing. This motor sits in the category of multirotor, which is not a problem since they will basically have the function of a multirotor, and will have the associated low-pitched propeller. In this case, the 13x5.5MR propeller is selected, the MR category being recommended by the manufacturer instead of the usual E (Electric). This motor and propeller combination is capable of producing 31.5 N of thrust at approx. 8700 RPM while ascending (the UAV) at a constant rate of 0.5 m/s. This gives the maximum output power with a 6 cell Li-Po battery.

With this, Objective *O1-A2* is achieved.

3.2. Battery Life

Each motor (twin wing motors seen as one) will have its own Li-Po battery pack to avoid circuitry that can upset the electronic components for navigation and other subsystems. For the front motor, a 6S LiPo battery with a capacity of 20 Ah will be used. Since each cell provides 3.2 V, the total cell voltage will be 19.2 V and knowing the power drawn by the propeller (max. = 1280 W), the current drawn can be obtained by Ohm's Law: 66.7 A. This current is lower than the maximum allowed by the motor. Dividing the current drawn by the capacity the discharge rate is obtained: 3.3C. Setting 70% as the maximum battery capacity that can be used per flight due to durability and safety concerns, the real flight time can be obtained. The resulting flight time is 12.7 minutes, which should be enough to complete the main mission tasks of the competition (Cargo Delivery, Climb and Glide). The wing motors are used less during a usual flight, so a good estimation would be a 6S LiPo battery with a capacity of 10 Ah, which gives a functioning time of around 6 minutes.

If the optional tasks were to be attempted, bigger batteries would be necessary.

3.3. Transition to Forward Flight Modelling & Simulation

In this section lies the most important part of the project, the one feature that makes the aircraft stand out amongst the majority of UAVs. That is, the transition from hover flight to forward flight. This stage is critical since it will decide the fate of the UAV. Any miscalculation can make the aircraft unstable and likely to crash. Therefore, it is vital to achieve a smooth transition.

To start with, the UAV is depicted with all the forces involved in the transition in *Figure 3.1*:

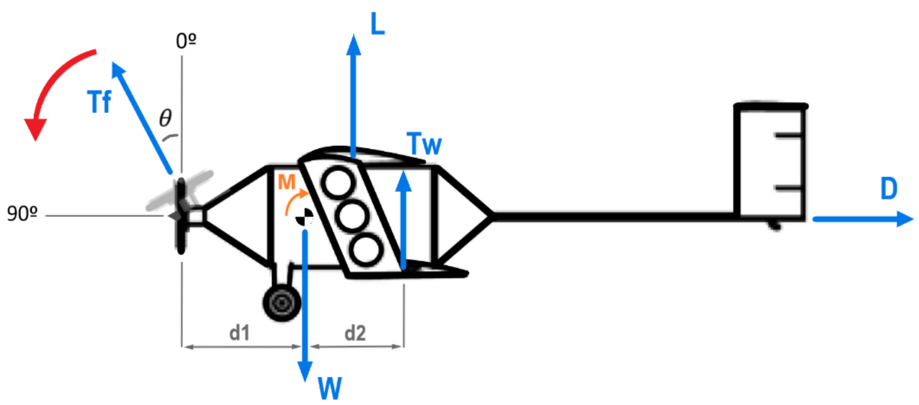

Figure 3.1: UAV representation and forces involved in the transition

Now, let us present the forces and parameters represented in *Figure 3.1* in the table below, together with valuable information to be accounted for from now on:

Force/Parameter	Description	Information
L	Total lift force	It is the sum of the lift force of the top wing and the bottom wing. Its application point lies in the midpoint of the quarter chord of both wings.
D	Drag force	It is horizontal (AoA = 0º) and aligned with the center of gravity. Therefore, it does not create any moment.
Tf	Front motor thrust	As the front motor is tilted with an angle theta, so does the thrust line. This creates a vertical and a horizontal component.
Tw	Wing motors thrust	It is the sum of the thrust produced by the twin wing motors. It points in the vertical direction and thus only has a vertical component unless there is an input angle of attack.
W	Weight of the UAV	It is given by the product of the UAV's mass and the gravity acceleration constant. Its application point is the center of gravity.
θ	Angle theta	It is the tilting angle of the front motor. In the transition it is limited to the range 0-90º, but the real range is 0-95º (pitch control).
d1	Distance 1	It is the distance in horizontal direction between the front motor and the center of gravity.
d2	Distance 2	It is the distance in horizontal direction between the center of gravity and the wing motors.
M	CG Moment	It is total moment about the center of gravity. It is composed by the moment generated by the lift, the wing motors thrust and the vertical component of the front motor thrust. It shall be equal to zero at all times to maintain the aircraft's attitude during the transition.

Once the forces are stablished, let us present the equations involved. Let us assume y is the vertical direction, positive upwards; and x is the horizontal direction, positive in the direction of the UAV's heading. The equations are:

$$\sum F_y = 0 \rightarrow T_f \cos(\theta) + T_w + L - W = 0 \qquad Equation\ 1$$

$$\sum M = 0 \rightarrow T_f \cos(\theta)\, d1 - T_w\, d2 = 0 \qquad Equation\ 2$$

$$\sum F_x = m\, a \rightarrow T_f \sin(\theta) = m\, a \qquad Equation\ 3$$

Equation 1 and *Equation 2* are equations of equilibrium, the former equilibrium of forces in the vertical direction and the latter equilibrium of moments about the center of gravity. On the other hand, Equation 3 is an equation of motion, and it will determine the acceleration, speed and position of the UAV as it transitions.

During the transition, the front motor is tilted from the starting point (vertical) with an increasing tilting angle theta. This will also tilt the front motor thrust line, creating both a vertical and a horizontal component of thrust. The increasing horizontal component will provide an acceleration in the x direction that will make the UAV start moving forward. As it starts gaining speed, it will start producing lift, proportionally to the square of speed as seen in *Equation 4*. In the same way, drag becomes increasingly important with speed, as seen in *Equation 5*.

$$L = \frac{1}{2}\rho\, S\, V^2 C_L \qquad\qquad Equation\ 4$$

$$D = \frac{1}{2}\rho\, S\, V^2 C_D \qquad\qquad Equation\ 5$$

At the same time, the vertical component of the front motor thrust will decrease, affecting the equilibrium of forces in the y direction and the equilibrium of moments. This can be solved either by increasing the front motor thrust proportionally or decreasing the wing motors thrust in an equal manner. Strictly, the latter alternative does not satisfy *Equation 1* (equilibrium of forces in the vertical direction), but a slow initial change of the tilting angle theta will result in a minimum altitude loss that is quickly compensated by the lift as the UAS gains speed. As the front motor is further tilted, the aircraft will keep accelerating, the lift will increase accordingly, and the wing motor thrust will be reduced until its contribution to lift is no longer necessary to maintain the UAS aloft. When this occurs, the wing motors are switched off (not exactly, min. RPM to increase circulation) and the UAS has reached the transition speed. For this project, the transition speed is that at which the aircraft is able to generate just enough lift to counter its weight. At this moment, the transition from hover to forward flight is achieved.

This transition was implemented and simulated in Matlab, gathered up in the program "*algorithm.m*". The code is designed in the following way. First of all, all the relevant data is inputted. This includes all UAV geometry parameters, mass distributions, aerodynamic coefficients, predefined thrust, conditions to be met, etc. Secondly, all the variables taking part of the equations that govern the transition are initialized. Before starting the loop, the time step, iteration time step and tilting angle theta step are set. Then, all the variables and equations are iteratively calculated as the tilting angle is increased and the wing motor thrust is decreased (both in steps) until either the UAV crashes or transitions to forward flight. That is, until the UAV reaches the transition speed. In this loop, the drag coefficient is a variable that is calculated iteratively with an external drag model function. After that, the data is plotted to compare the results obtained, and in an iterative but manual way, some conditions and parameters are changed until the transition is the smooth and safe.

For the sake of simplicity, the angle of attack has been kept constant and equal to zero. If the AoA were to be modified during the transition, a horizontal component of the wing motors thrust would appear and act along with the drag (for AoA greater than 0), and the tilting range of the front propeller would have to be increased on top of other problems that would arise.

With this, Objective *O2-A2* is mostly fulfilled, since the transition from forward flight back to hover has not been modelled yet. These plots are analyzed and discussed in the following section.

4. Results, Analysis and Discussion

In this section, the results of two different transition models are shown in the form of plots. The first model (*TRANSITION I*) the UAS is already in the air hovering at an altitude H and the transition takes place from there. The second model (*TRANSITION II*) starts the transition at the same time it takes off. This second model can be more interesting for the competition since it saves time.

It is of importance to note that the transition models assume a 2D trajectory, rejecting any possible sideways deviation.

4.1. Transition I

As mentioned above, this first model starts from hover and then transitions into forward flight. It can be seen in *Figure 4.1* that the UAV starts the transition from a height of 15 m. Then, it has a minimum drop in height (centimeters) due to the initial tilt, but it quickly recovers and starts gaining speed and climbing. The transition is achieved in 13.3 seconds, when the UAV is located approx. at distance of 60 m and a height of 19 m.

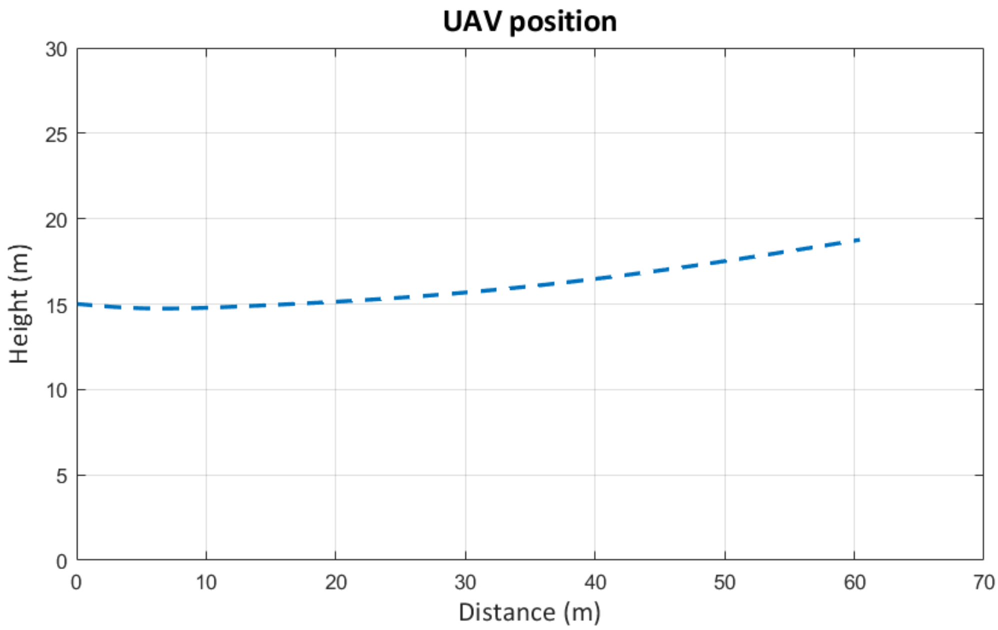

Figure 4.1: UAV position plot during transition (I).

In *Figure 4.2*, the forward speed is plotted against drag in an attempt to illustrate the drag model of the particular UAV. Once the UAV dimensions are completely constrained, it could be done a polynomial fitting to obtain a curve that can be used later to simplify calculations.

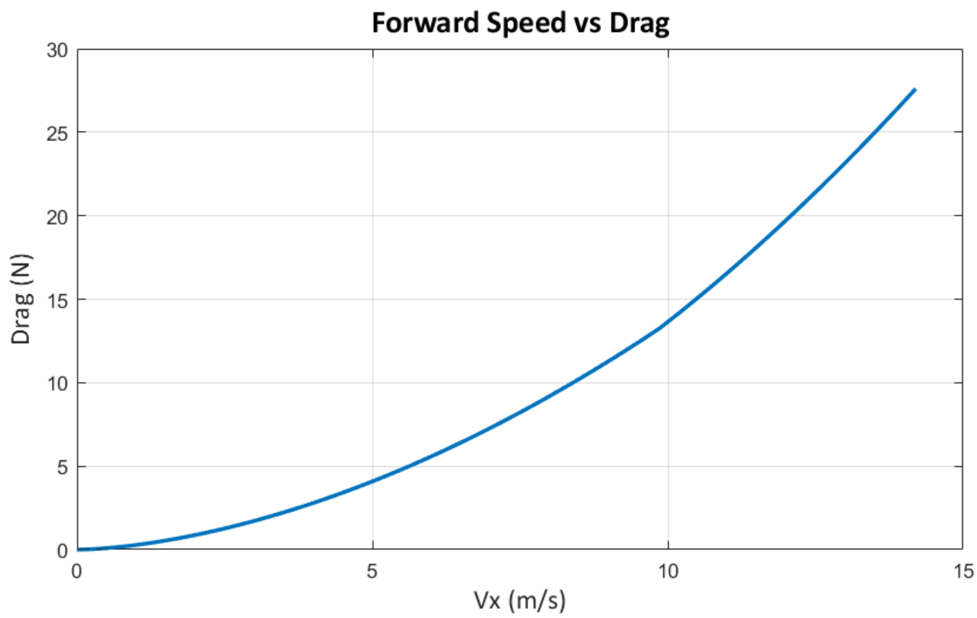

Figure 4.2: UAV position plot during transition (I).

Next, the lift and also the tilting angle theta are depicted against time. This is seen in *Figure 4.3*. It can be observed the quadratic increase in lift as the velocity increases, up to the point where it matches the weight of the aircraft (black line). Also, it can be seen the increasing rate of change of theta with time by steps, which directly affects the horizontal component of thrust and therefore the speed and lift of the UAV.

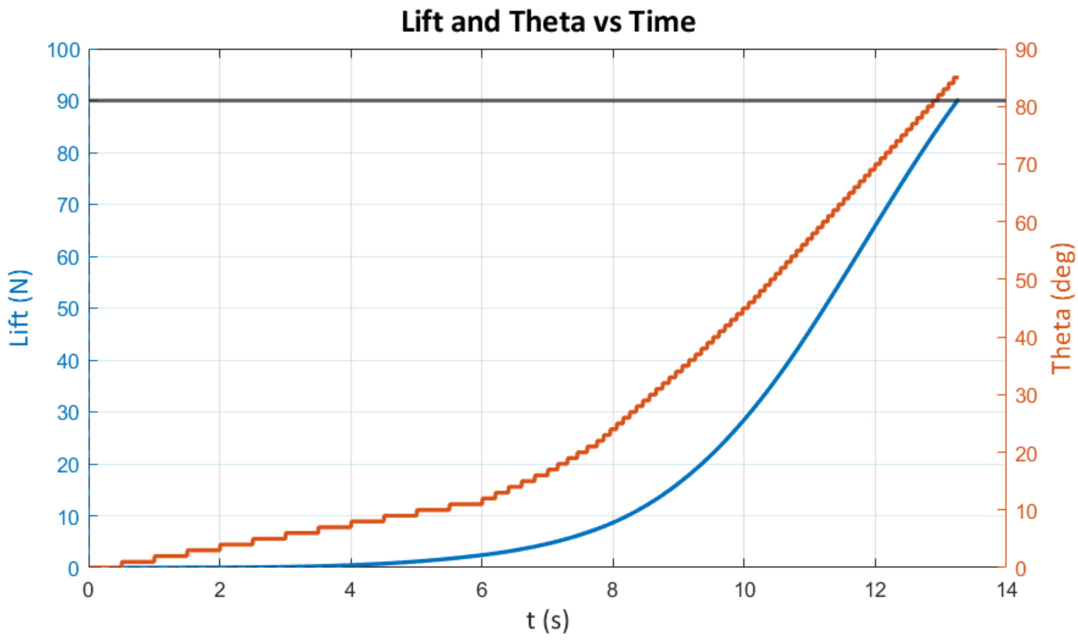

Figure 4.3: UAV position plot during transition (I).

In a similar manner, *Figure 4.4* shows the forward velocity and theta plotted against time. The same conclusions can be obtained as before. Something to note is that the transition is achieved before the front motor is fully horizontal (at around theta = 85 deg).

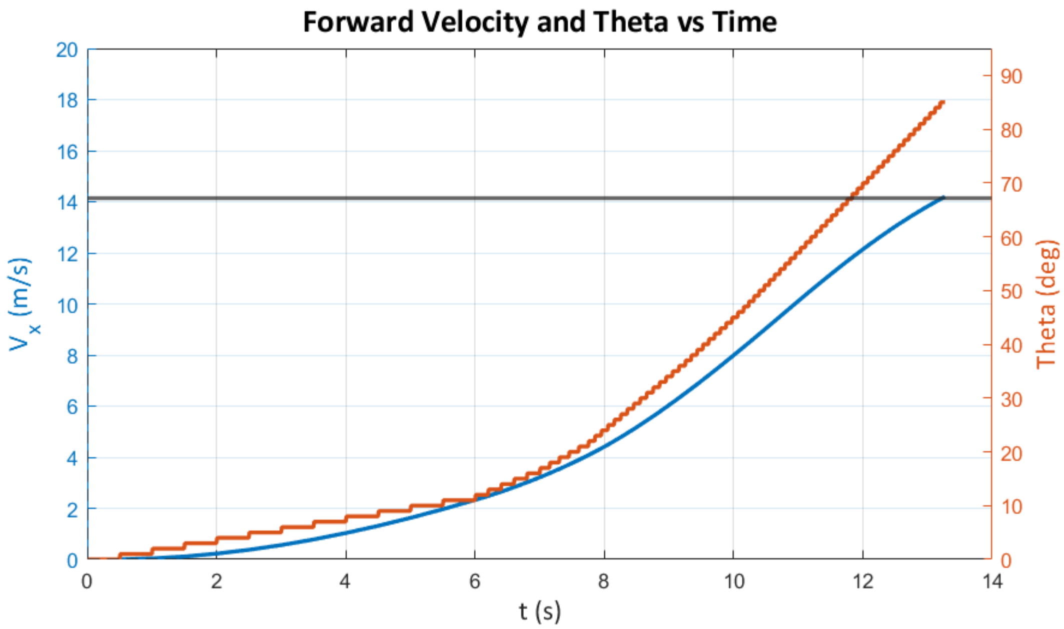

Figure 4.4: UAV forward velocity and theta plot against time during transition (I).

Figure 4.5 shows how the forward thrust and the wing thrust changes with theta. As it was established in previous sections, the forward thrust is kept constant while the wing thrust is reduced in order to compensate for the moment loss and the increasing lift.

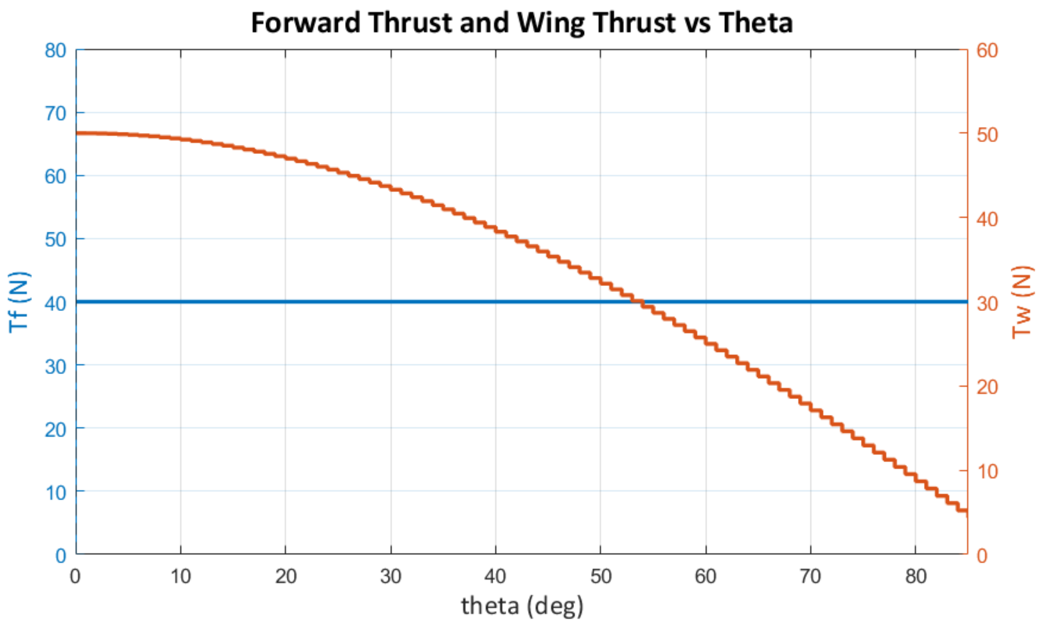

Figure 4.5: UAV forward thrust and wing thrust plot against theta during transition (I).

Finally, *Figure 4.6* shows the most important plot to understand what the transition model does. Going back to *Equation 1*, this plot represents the equilibrium of forces in the vertical direction. Initially and approximately during the first 4 seconds, all the vertical force to sustain the UAV is produced by the thrust of the three motors. As the front motor is tilted, the vertical component is decreased and the wing motors thrust is decreased accordingly. The speed in the horizontal direction keeps increasing, and the lift becomes noticeable and starts increasing rapidly until it equals the UAV weight. At this point, the vertical thrust of the motors is null, and the transition has been achieved. The total vertical force is approx. equal to zero until t = 10 s, when it increases up to 5-7 N. This is corresponded with the small climb of the UAV.

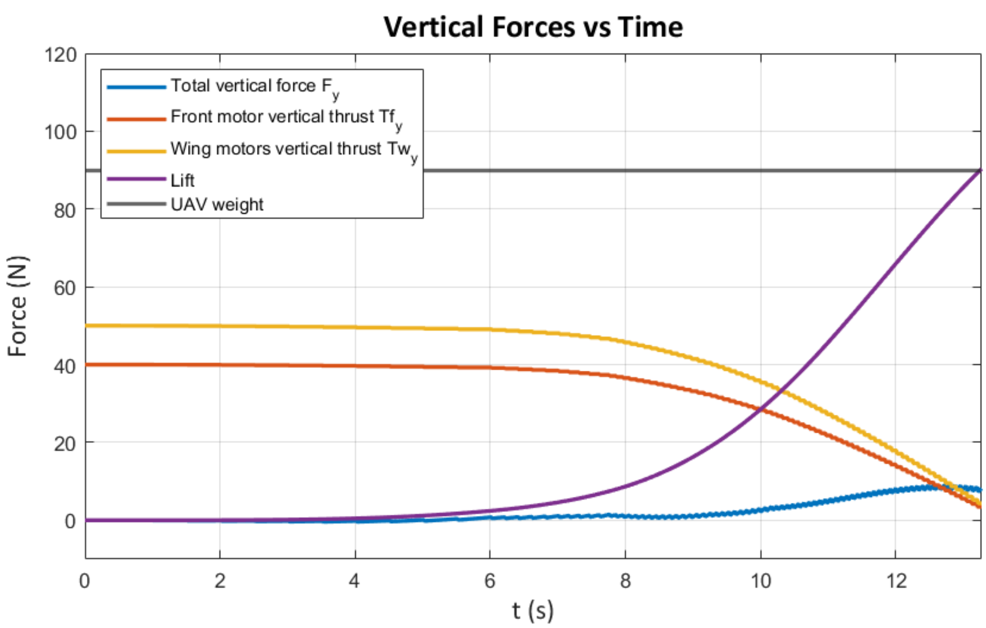

Figure 4.6: UAV vertical forces plot against time during transition (I).

4.2. Transition II

The second model starts from the ground, and then it transitions into forward flight while taking-off. It can be seen in *Figure 4.7* that the UAV starts the transition from a height of 0 m. The transition is achieved in 12.95 seconds, when the UAV is located approx. at distance of 57 m and a height of 17 m. This is practically the same time it took *TRANSITION I*, and it includes the take-off too. It can be observed then, the great advantage this model shows when it come to the competition.

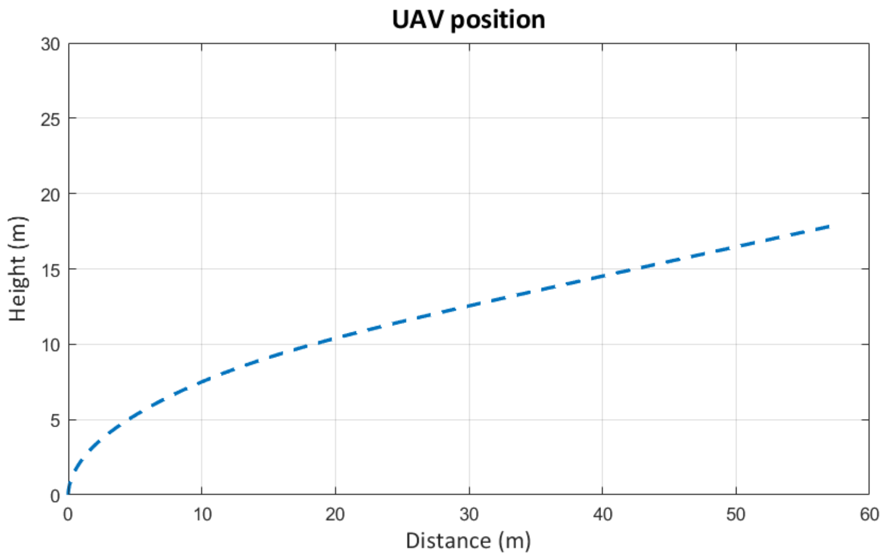

Figure 4.7: UAV position plot during transition (II).

Figure 4.8 is very similar to *Figure 4.9*, but with the difference that the total vertical force is always greater than zero (3-5 N initially) in order to take off.

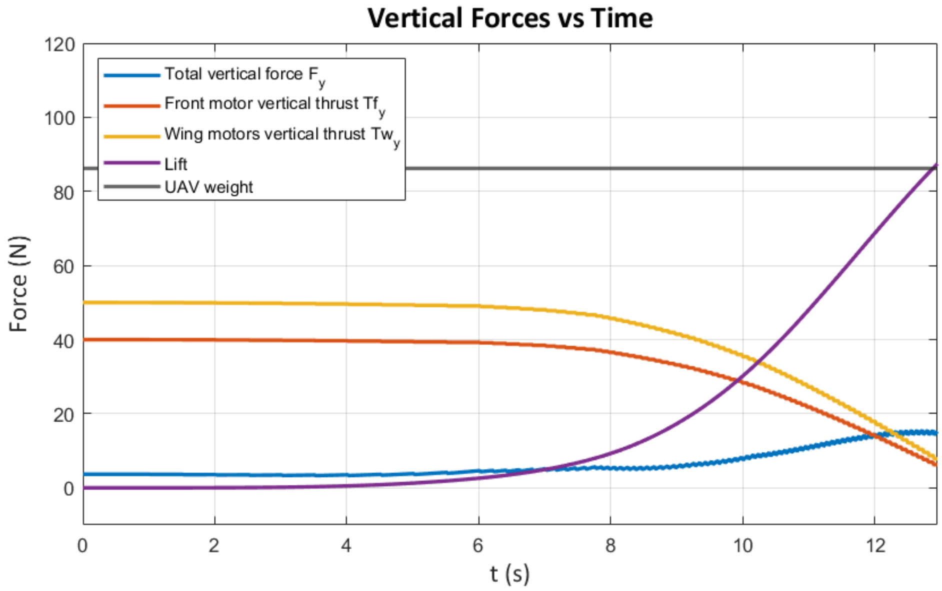

Figure 4.8: UAV vertical forces plot against time during transition (II).

This concludes the analysis of results.

5. Conclusions & Future Work

To conclude, the project can be considered a success since two out of three aims were met (*Aim 1* and *Aim 2*). An initial research was carried to learn the state of the art. Unfortunately, little was directly applicable to type of aircraft shown in this paper: a VTOL biplane UAS with a tilting front motor and two wing embedded motors. Consequently, most of the project was carried out with the previous knowledge in the aerospace field. A code to model the transition has been developed from scratch, and the results have shown the possibility of a transitioning UAV becoming real. Still, many factors that affect this transition are not yet constrained e.g. the complete geometry of the UAV and others, so the transition will have to be recalculated when the time comes.

Future work will mainly consist in perfecting the transition model and design a not so similar model to transition from forward flight back to hover. Then, the code shall be integrated in the yet to be investigated autopilot of the UAV. As the autopilot will have sensors continuously reporting positioning, speed, acceleration, etc. the drag will be calculated onboard and the drag model of the code will no longer be necessary. Further work may include CFD simulations to analyze the extent to which the embedding of the wing propellers affects lift (probably to a small extent); the development of a STOL approach for take-off (3rd approach); and of course, flight tests.

Aim 3 will be achieved in the next few months. When the construction phase takes place (Objective *O1-A3*) and the autopilot is integrated (Objective *O2-A3*), we will be ready to participate in the IMechE UAS Challenge, and hopefully present a super innovative UAS that meets or exceeds the competition requirements.

6. References

Abdessameud, A., & Tayebi, A. (2013). Motion Coordination for VTOL Unmanned Aerial Vehicles. In M. J. Grimble & M. A. Johnson (Eds.), *ADVANCES IN INDUSTRIAL CONTROL* (p. 24). Springer.

Bestaoui Sebbane, Y. (2018). *Intelligent Autonomy of Uavs: Advanced Missions and Future Use* (2nd ed., p. 1). Chapman and Hall/CRC. https://doi.org/10.1201/b22485

Dalamagkidis, K., Valavanis, K.P., & Piegl, L.A. (2009). On Integrating Unmanned Aircraft Systems into the National Airspace System. In S. G. Tzafestas (Ed.), *INTELLIGENT SYSTEMS, CONTROL, AND AUTOMATION: SCIENCE AND ENGINEERING* (p. 1). Springer Science+Business Media.

Kowal, H.J. (2002). Advances in thrust vectoring and the application of flow-control technology. Canadian Aeronautics and Space Journal, 48(2), 145-147. https:// doi.org/10.5589/q02-020

Kuhn, R.E., Margason, R.J., & Curtis, P. (2006). *Jet Induced Effects: The Aerodynamics of Jet and Fan Powered V/STOL Aircraft in Hover and Transition*. American Institute of Aeronautics and Astronautics, Inc.

Roberts, A.D. (2007). Attitude estimation and control of a ducted fan VTOL UAV [Master Dissertation, Lakehead University].
http://knowledgecommons.lakeheadu.ca/handle/2453/3699